Divergent Stereochemical Outcomes in the Insertion of Donor/Donor Carbenes into the C–H Bonds of Stereogenic Centers

Sarah N. Dishman, Croix J. Laconsay, James C. Fettinger, Dean J. Tantillo, and Jared T. Shaw*

Department of Chemistry, University of California, One Shields Avenue, Davis, California 95616, USA

C–H insertion, Donor/Donor carbene, Stereoselective, Density Functional Theory

ABSTRACT: Intramolecular C–H insertions with donor/donor dirhodium carbenes provide a concise and highly stereoselective method to set two contiguous stereocenters in a single step. Herein, we report the insertion of donor/donor carbenes into stereogenic carbon centers allowing access to trisubstituted benzodihydrofurans in a single step. This study illuminates, for the first time, the stereochemical impact on the carbene center and delineates the structural factors that enable control over both stereogenic centers. Sterically bulky, highly activated C–H insertion centers exhibit high substrate control yielding a single diastereomer and a single enantiomer of product regardless of the catalyst used. Less bulky, less activated C–H insertion centers exhibit catalyst control over the diastereomeric ratio (dr), where a single enantiomer of each diastereomer is observed with high selectivity. A combination of experimental studies and DFT calculations elucidate the origin of these results. First, hydride transfer from the stereogenic insertion site proceeds with high stereoselectivity to the carbene center, thus determining the absolute configuration of the product. Second, the short lived zwitterionic intermediate can diastereoselectively ring-close by a hitherto unreported S_E2 mechanism that is either controlled by the substrate or the catalyst. These results demonstrate that donor/donor carbenes undergo uniquely stereoselective reactions that originate from a stepwise reaction mechanism, in contrast to the analogous concerted reactions of carbenes with one or more electron-withdrawing groups attached.

INTRODUCTION

The insertion of metal carbenes into C–H bonds enables the efficient and stereoselective synthesis of a wide array of complex organic molecules.[1] Most metal carbenes derive their high reactivity from having one or more electron-withdrawing groups to confer high electrophilicity. Carbenes with one electron-donating group (e.g. a phenyl or styrenyl) and one electron-withdrawing group are denoted as "donor/acceptor" carbenes and exhibit exquisite regio- and stereoselectivity in intermolecular insertions.[2–4] More recently carbenes lacking any electron-withdrawing groups, i.e., "donor/donor carbenes" have been employed in intra- and intermolecular reactions.[5–9] The reduced electrophilicity of donor/donor carbenes enables a high degree of functional group tolerance and the accessibility of generating the diazo carbene precursors *in situ* provides excellent scalability and safety.[7,10] Herein, we report C–H insertion reactions of donor/donor carbenes into stereogenic carbon centers which allow for stereoselective access to trisubstituted benzodihydrofuran cores in a single step. For the first time, this study highlights the stereochemical impact on the carbene center and delineates the structural factors that enable control over both stereogenic centers. This facile method to generate trisubstituted benzodihydrofuran cores enables the asymmetric synthesis of multiple classes of natural products, patented biologically active small molecules, and their analogs, to be rapidly synthesized (Figure 1).[11–17]
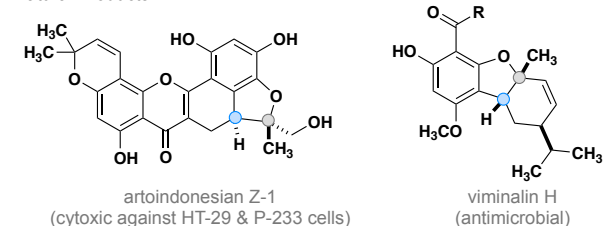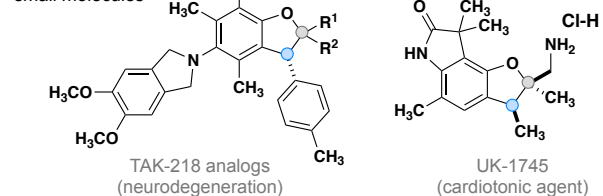

Figure 1. Natural products and patented small molecules containing trisubstituted benzodihydrofuran cores.

Previous work by Taber[18] and Doyle[19] used chiral C–H insertion centers and acceptor-substituted carbenes to create selectivity models for their respective systems. Taber demonstrated that the stereochemistry of the C–H insertion site was retained and attributed this observation to a concerted mechanism (Figure 2A). The stereochemical

outcome of the carbene center was not evaluated due to the high enolizability of the product and its subsequent decarboxylation. Similarly, Doyle used a chiral substrate and demonstrated retention of configuration as well as catalyst-controlled regiochemistry (Figure 2A). Again, the fate of the carbene center was not examined because that carbon was non-stereogenic in the product. To date, no studies have examined the stereochemical impact of insertion reactions of donor/donor carbenes. While acceptor-substituted carbenes undergo C–H insertion by a concerted mechanism, the stepwise mechanism[7] of donor/donor carbenes suggests that the formation of two new stereogenic centers may be influenced by both the substrate and the catalyst (Figure 2B).
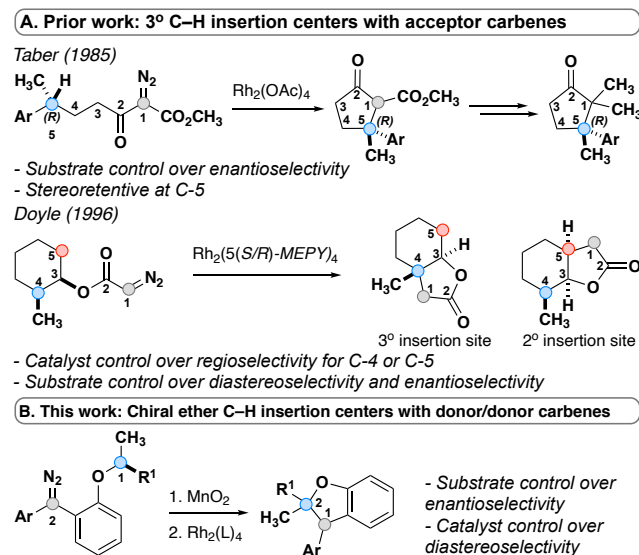

Figure 2. A) Prior work- tertiary C–H insertion centers with acceptor carbenes. B) This work- donor/donor carbenes with chiral, tertiary C–H insertion centers.

RESULTS AND DISCUSSION

The level of stereocontrol the substrate and catalyst impart on the C–H insertion reaction was assessed with two ether substrates and two catalysts. Ethers **1** and **2** (Figure 3) each have a stereogenic insertion site with varying levels of reactivity based on the different stabilities of the oxocarbenium intermediate resulting from hydride transfer. Substrate **1** has a benzylic site that is highly reactive toward C–H insertion and a *p*-cyano group on the phenyl donor core to enable subsequent derivatization for crystallography and separation by chiral HPLC. Notably, previous work by our group shows that electronic variation of the phenyl donor core doesn't affect the enantiomeric ratio (er) significantly.[7] The chiral homoallylic ether, substrate **2,** is less activated toward C–H insertion because there is no stabilization of the cation intermediate via resonance. The homoallylic ether also enabled better separation by chiral HPLC and the opportunity to obtain a crystalline derivative. Each C–H insertion reaction could potentially yield two diastereomers and their respective enantiomers. Both racemic and enantiopure substrates were used with chiral dirhodium catalysts (*R*-**3** and *S*-**3**) as

well as the achiral catalyst Rh₂(mes-CO₂)₄ (**4**) (Figure 3). The experimental data collected from multiple substrate and catalyst pairings enabled stereochemical trends to be identified and studied further using DFT calculations (*vide infra*).
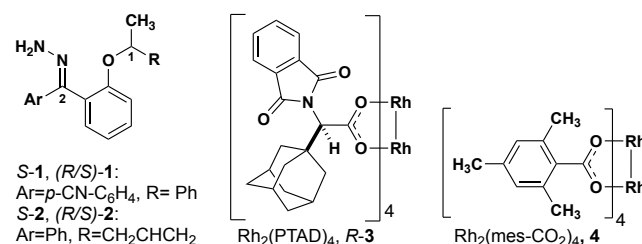

Figure 3. Structures of hydrazone precursors and commonly used dirhodium catalysts with donor/donor carbene C–H insertion systems

Initial studies involved substrate **1**, containing a highly activated and bulky C–H insertion center substituted with methyl and phenyl groups. Both racemic **1** and enantiopure **1** yielded the benzodihydrofuran product as a single cis diastereomer (**5a**, Table 1, entries 1-3) irrespective of which catalyst was used. The enantioselectivity followed a similar trend where racemic **1** provided racemic **5a** and enantiopure **1** gave a single enantiomer of **5a** in 97:03 er (Table 1, entries 4-6) regardless of the catalyst employed in the reaction. Therefore, these substrates with highly activated, sterically occluded C–H insertion centers elicit highly stereoselective substrate-controlled C–H insertion reactions.

Table 1. Alkyl/Aryl Stereogenic Insertion Centers
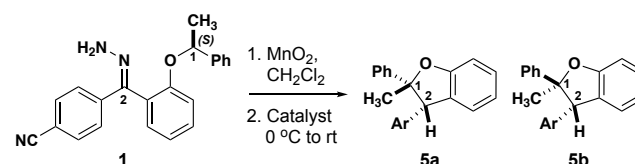
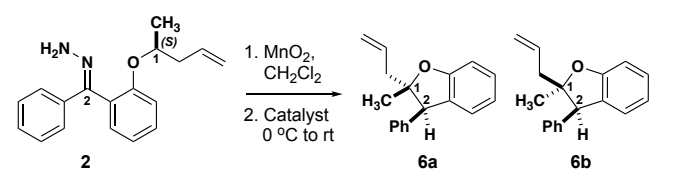| Entry	SM	Catalyst	dr[a] 5a:5b	er[b] (4a) (S,S):(R,R)	Yield (%)
1	(*R,S*)-**1**	*R*-3	>95:5	49:51	68
2	(*R,S*)-**1**	*S*-3	>95:5	49:51	65
3	(*R,S*)-**1**	4	>95:5	49:51	65
4	(*S*)-**1**	*R*-3	>95:5	97:03	82
5	(*S*)-**1**	*S*-3	>95:5	97:03	71
6	(*S*)-**1**	4	>95:5	97:03	76

[a]dr determined by ^{1}H NMR analysis of unpurified reaction mixtures. [b]er determined by chiral HPLC. [c]Absolute stereochemistry confirmed by X-ray crystallography.

The diastereoselectivity of the reaction with **1** is not influenced by the structure of the catalyst whereas the enantioselectivity is dictated by the configuration at the carbon undergoing insertion. These results are consistent with those of Taber and Doyle in that the configuration of insertion site of (S)-**1** is retained in product **5a**, i.e., consistent with a concerted C–H insertion mechanism. The

differential results from (*R,S*)-**1** and (*S*)-**1** suggest that the configuration at the insertion site (C-1) dictates the configuration at (C-2) during the insertion reaction. These data do not rule out a highly stereoselective stepwise mechanism.

Based on the results above, a less activated, less bulky C–H insertion center substituted with methyl and homoallylic groups (**2**) was examined to see if diastereo- or enantiocontrol over the reaction differed from **1** (Table 2). Interestingly, the C–H insertions reactions of these less activated substrates showed drastically different stereoselectivity trends compared to the alkyl/aryl substrates. Racemic **2** yielded a 47:53 and 48:52 dr of **6a**:**6b** with *R*-**3** and *S*-**3** respectively (Table 2, entries 1-2). There was a slight enrichment towards the trans diastereomer (**6a**) with **4** yielding a 57:43 dr (Table 2, entry 3). Strikingly, when the er was measured the chiral catalysts generated each diastereomer of **6** in high er (Table 2, entries 1-2), while the achiral catalyst yielded racemic mixtures of each diastereomer of **6**. While substrate (*R/S*)-**1** led only to racemic products, (*R/S*)-**2** can be steered toward enantio-enriched products with the chiral catalysts.

Table 2. Alkyl/Alkyl Stereogenic Insertion Centers

Entry	SM	Catalyst	dr[a] 6a:6b	er[b]-6a (S,R): (R,S)	er[b]-6b (R,R): (S,S)	Yield (%)
1	(*R/S*)-**2**	*R*-3	47:53	91:09	86:14	70
2	(*R/S*)-**2**	*S*-3	48:52	11:89	16:84	68
3	(*R/S*)-**2**	4	57:43	49:51	50:50	91
4[c]	(*S*)-**2**	*R*-3	86:14	99:01	99:01	77
5	(*S*)-**2**	*S*-3	10:90	74:26	99:01	75
6	(*S*)-**2**	4	53:47	98:02	99:01	58

[a]dr determined by ^{1}H NMR analysis of unpurified reaction mixtures. [b]er determined by chiral HPLC. [c]Absolute stereochemistry confirmed by X-ray crystallography.

The results with (*S*)-**2** were even more striking. Treatment of this substrate with *R*-**3** resulted in preferential formation of cis benzodihydrofuran **6a** (Table 2, entry 4) with high enantioselectivity. Use of the same substrate with *S*-**3** resulted in inverted diastereoselectivity *with the same enantiomeric preference as the reaction with* R-**3** (Table 2, entry 5)*!* The eroded enantioselectivity for the formation of **6a** in this case highlights the mismatch in stereochemical preference between the substrate and the catalyst. Finally, the insertion of (*S*)-**2** with achiral catalyst (**4**) showed little diastereoselectivity while retaining the high substrate-

induced enantioselectivity (Table 2, entry 6). On one hand, these results demonstrate that the stereogenic center undergoing insertion controls the magnitude and orientation of enantioselectivity for both newly formed stereogenic centers in the product. The catalyst, on the other hand, can have a strong influence on the diastereoselectivity, and *R/S*-**3** is a privileged catalyst scaffold for this system.[7] These results are consistent with a highly stereoselective hydride transfer step that is followed by a diastereoselective ring closure that can be controlled by the configuration of the catalyst.

To investigate the C–H insertion mechanism leading to **6** and delve further into the origins of the observed stereocontrol, we turned our attention to computational studies. Density functional theory (DFT) calculations have previously aided our study of C–H insertion mechanisms of donor/donor carbenes.[7] However, unlike previous DFT explorations of similar reactions in which the Rh catalyst can be reasonably modeled with $Rh_2(OAc)_4$, or even $Rh_2(HCO_2)_4$,[20] we could only adequately investigate the current mechanistic question by modeling the insertion reaction of **6** within the chiral cavity[21,22] of either $Rh_2(R$-PTAD$)_4$ or $Rh_2(S$-PTAD$)_4$. Given the size of the *N*-phthalimido and adamantyl ligands on $Rh_2(R$-PTAD$)_4$ (weighing in at 219 atoms and 940 electrons), and its concomitant computational cost, we reasoned that truncating the adamantyl groups to methyl groups struck a sensible balance between mechanistic insight and cost with the modeling capabilities at our disposal.[21,22]

A stepwise mechanism containing a short lived zwitterionic intermediate was found for the reactions of substrate **2**, similar to that previously proposed for C–H insertions of donor/donor carbenes with primary, achiral insertion sites (see computational SI for details).[7] For clarity, the mechanism for formation of one enantiomer of the major diastereomer is shown in Figure 3 (See SI for detailed reaction profiles for formation of the other diastereomer and its enantiomer are reported). First, addition of the chiral catalyst results in a tetrahedral intermediate (**11**) with N_2 poised to leave. The barrier to extrude nitrogen is low and this process is predicted to be highly exergonic, forming one major rotamer of Rh carbene (**8**). From **8**, an initial hydride-shift from C-1 to C-2 is followed by an S_E2 C–C bond closure step to yield the major product (**6a**).[23] The hydride transfer occurs with high stereochemical fidelity, accounting for the high selectivity for the newly formed stereogenic center at C-2. The diastereomeric ratio observed is hypothesized to be due to the major oxocarbenium ion intermediate (**9**) rotating about the C_{aryl}–O bond to expose one prochiral face, preferentially exposing one prochiral face based on the configuration of the catalyst. Although our computed mechanism is formally stepwise, the C–H insertion event can be considered to border the realm of a concerted, highly asynchronous mechanism (see SI Figure 3).[24]
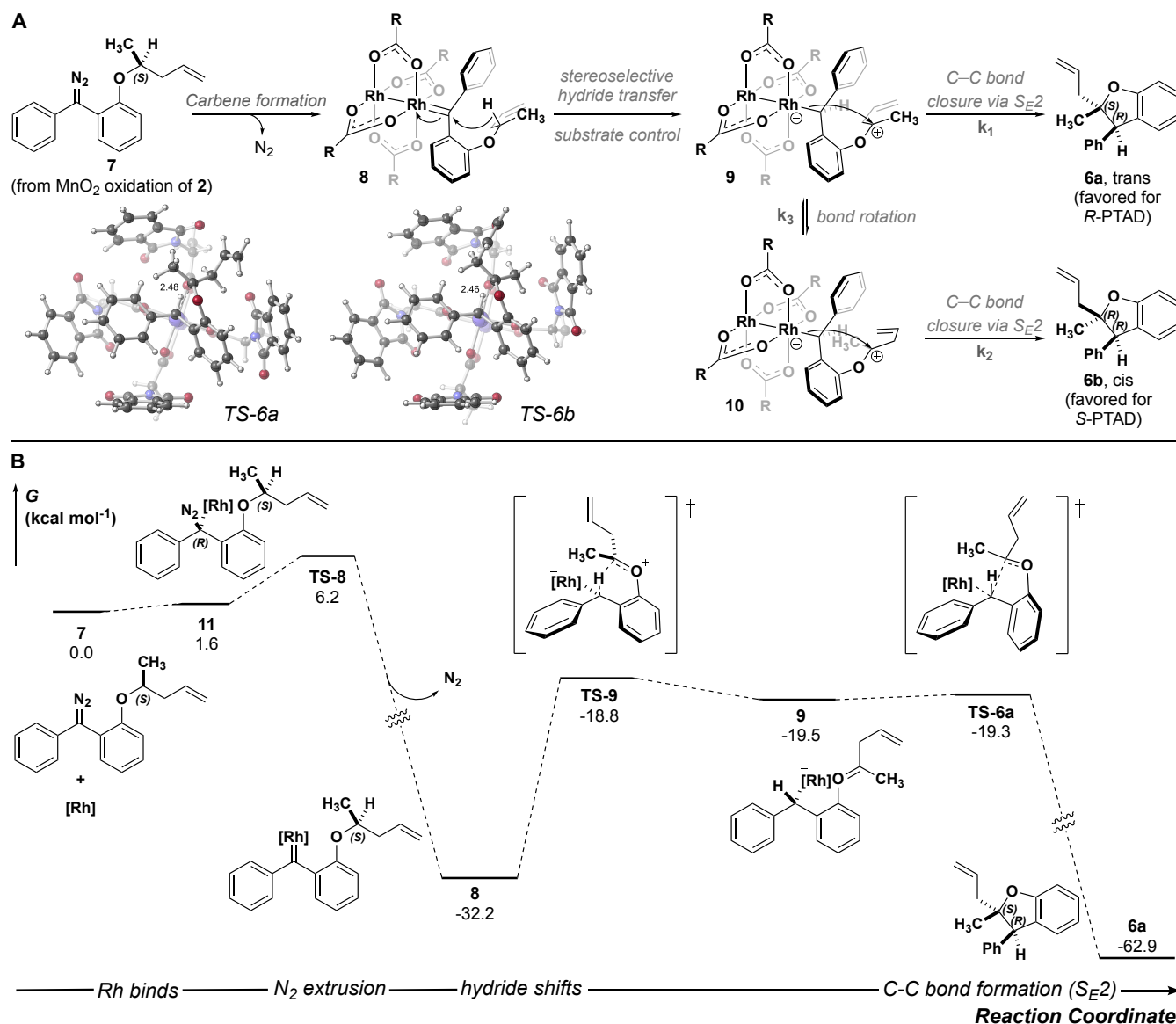
Figure 4. A) Arrow pushing mechanism and S_E2 transition-state structures leading to 6a and 6b. B) Reaction energy profile computed with DFT at the PCM(CH$_2$Cl$_2$)-B3LYP-D3(BJ)/SDD[6-31+G(d,p)]//PCM(CH$_2$Cl$_2$)-B3LYP-D3(BJ)/LANL2DZ[6-31G(d)] level of theory; [Rh] = Rh$_2$(R-PTAD)$_4$.

Although we successfully identified transition states leading from **9** to **6a** and from **10** to **6b** (SI Figures 4-5), the transition state for **9** to **10** remains elusive. The observed 85:15 ratio results from the relative energy of these two transition states, as well as the interconversion of **9** to **10**. While it is difficult to disentangle the exact influence of these three transition states on diastereoselectivity, the data are consistent with an oxocarbenium ion whose stereochemical fate is determined by the catalyst. Small perturbations resulting from factors not explicitly modeled here, e.g., explicit solvent effects, deviations in the chiral crown structure, or non-statistical dynamic effects, could account for issues in delineating these three steps' effect on the diastereoselectivity.[25-30]

This stepwise pathway can be used to hypothesize a similar mechanism for **5a** (Figure 5). Oxidation of (S)-**1** to diazo followed by addition of catalyst will form Rh carbene **12**. This intermediate will undergo the same highly stereoselective hydride transfer to form a single **9**, rotating about the C$_{aryl}$–O bond in **13** to expose the other prochiral
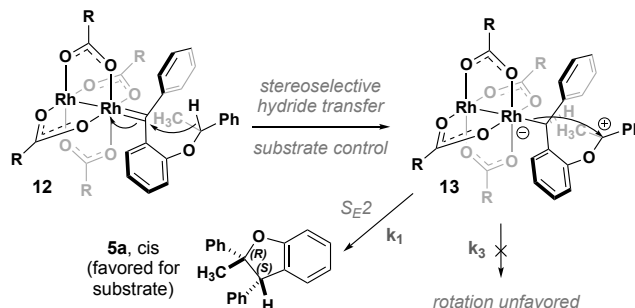

**Figure 5.** Proposed arrow pushing mechanism leading to **5a**.

oxocarbenium ion intermediate (**13**). Unlike intermediate face of the oxocarbenium ion is likely kinetically unfavorable due to increased steric bulk, contributing to a high energic cost to rotate in the chiral cavity. Therefore, **13** rapidly closes to form a new C–C bond by an S_E2 mechanism yielding **5a** as the single enantiomer and single diastereomer of product. The computed pathway for the carbene intermediate of substrate **1** reacting with $Rh_2(OAc)_4$ supports a stepwise mechanism for C–H insertion event: the intermediacy of an oxocarbenium ion results from hydride transfer that proceeds to **5a** through an S_E2 mechanism, similar to what is observed for **9** proceeding to **6a**.

Table 3. Varying electronic activation and steric bulk at the C–H insertion center
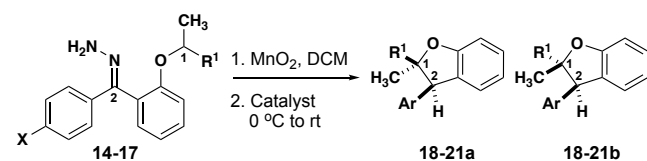
Entry	Product	X	R^1	Catalyst	dr^a (a:b)	Yield (%)
1^b	18	H	Et	*R*-3	46:54	85
2^b	18	H	Et	*S*-3	46:54	87
3^b	18	H	Et	4	58:42	85
4^b	19	CN	*i*-Pr	*R*-3	38:62	74
5^b	19	CN	*i*-Pr	*S*-3	35:65	76
6^b	19	CN	*i*-Pr	4	81:19	70
7^b	20	H	*c*Pr	*R*-3	15:85	93
8^b	20	H	*c*Pr	*S*-3	15:85	91
9^b	20	H	*c*Pr	4	32:68	44
10^b	21	H	Ph	*R*-3	>95:5	70
11^b	21	H	Ph	*S*-3	>95:5	80
12^b	21	H	Ph	4	>95:5	76

^{a}dr determined by ^{1}H NMR analysis of unpurified reaction mixtures. ^{b}assigned diastereomers determined from analogous compound NMR shifts, see SI.

This mechanistic model enables rapid assessment of new substrates. If a racemic substrate results in low diastereoselectivity with an achiral catalyst, as was the case with **2**, we predict that it is possible to observe high diastereoselectivity with a single enantiomer of starting material and a chiral catalyst. If, on the other hand, a substrate exhibits high diastereoselectivity under the same circumstances, we predict it will probably be *impossible* to favor the minor diastereomer under any circumstances. In all cases, high enantioselectivity for both diastereomers can be expected to result from an enantiomerically pure substrate regardless of catalyst chirality. Four additional substrates are illustrative of these generalizations (Table 3). An *n*-alkyl substrate (**14**, R=Et) behaves much like **2**, exhibiting little substrate control, offering the opportunity for catalyst control. Substrate **17**, which is analogous to **1**, exhibits high substrate control. A branched alkyl substrate

(**15**, R=*i*-Pr) is intermediary, with a substrate preference that is opposite to what is preferred by either enantiomer of catalyst **3**. Finally, **16** (R=*c*Pr) exhibits a slight preference for one diastereomer with catalyst **4** that is enhanced by either enantiomer of catalyst. It is possible in the cases of **15** and **16** that a particular substrate/catalyst pairing will enable high diastereoselectivity, but the inherent substrate control exhibited by the achiral catalyst suggests that favoring the other diastereomer will be more challenging than it is for **2** and **14**.

CONCLUSION

In summary, we have developed a method and stereochemical rationale for intramolecular C–H insertion reactions with donor/donor carbene systems having chiral ethers. This enables the generation of two contiguous stereogenic centers in a single step, yielding a trisubstituted benzodihydrofuran core. Exploration of chiral substrates with two enantiomers of a chiral catalyst revealed stereoselectivity patterns not observed with other types of carbene C–H insertion systems. High enantioselectivity can be achieved and controlled based on the enantiomer of starting material used. For sterically occluded and highly activated C–H insertion centers, high diastereoselectivity emerges from substrate control, irrespective of the catalyst used. Less sterically demanding and less activated C–H insertion centers exhibit high diastereoselectivity that is controlled based on the enantiomer of catalyst employed in the reaction. Our DFT studies with a truncated variant of the chiral $Rh_2(R\text{-PTAD})_4$ catalyst demonstrate that the highly stereoselective hydride transfer controls enantioselectivity outcomes, whereas a zwitterionic intermediate undergoes diastereoselective ring closure through an S_E2 mechanism. These studies demonstrate that donor/donor carbenes are capable of unique levels of stereocontrol not previously seen with carbenes appended with one or more electron-withdrawing group.

ASSOCIATED CONTENT

Supporting Information

The Supporting Information is available free of charge on the ACS Publications website.

Experimental details, characterization data, and spectra (PDF)

Computational data and procedures. All computed structures discussed in this manuscript can be found in the ioChem-BD repository[31] at the following DOI: https://doi.org/10.19061/iochem-bd-6-94 (PDF)

Crystallographic data for (*S,S*)-**4a** (cif)

Crystallographic data for (*S,R*)-**5a** (cif)

Crystallographic data for (*R,R*)-**5b** (cif)

AUTHOR INFORMATION

Corresponding Author

Jared T. Shaw — Department of Chemistry, University of California, Davis, Davis, CA 95616, United States; orcid.org/0000-0001-5190-493X; Email: jtshaw@ucdavis.edu

REFERENCES

(1) Abrams, D. J.; Provencher, P. A.; Sorensen, E. J. Recent Applications of C-H Functionalization in Complex Natural Product Synthesis. *Chem. Soc. Rev.* **2018**, *47* (23), 8925–8967.

(2) Doyle, M. P.; Duffy, R.; Ratnikov, M.; Zhou, L. Catalytic Carbene Insertion into C-H Bonds. *Chem. Rev.* **2010**, *110* (2), 704–724.

(3) Fu, J.; Ren, Z.; Bacsa, J.; Musaev, D. G.; Davies, H. M. L. Desymmetrization of Cyclohexanes by Site- and Stereoselective C–H Functionalization. *Nature* **2018**, *564* (7736), 395–399.

(4) Davies, H. M. L.; Liao, K. Dirhodium Tetracarboxylates as Catalysts for Selective Intermolecular C–H Functionalization. *Nat. Rev. Chem.* **2019**, *3*, 347–360.

(5) Jagannathan, J. R.; Fettinger, J. C.; Shaw, J. T.; Franz, A. K. Enantioselective Si-H Insertion Reactions of Diarylcarbenes for the Synthesis of Silicon-Stereogenic Silanes. *J. Am. Chem. Soc.* **2020**, *142* (27), 11674–11679.

(6) Cheung, W.-H.; Zheng, S.-L.; Yu, W.-Y.; Zhou, G.-C.; Che, C.-M. Ruthenium Porphyrin Catalyzed Intramolecular Carbenoid C-H Insertion. Stereoselective Synthesis of Cis-Disubstituted Oxygen and Nitrogen Heterocycles. *Org. Lett.* **2003**, *5* (14), 2535–2538.

(7) Lamb, K. N.; Squitieri, R. A.; Chintala, S. R.; Kwong, A. J.; Balmond, E. I.; Soldi, C.; Dmitrenko, O.; Castiñeira Reis, M.; Chung, R.; Addison, J. B.; Fettinger, J. C.; Hein, J. E.; Tantillo, D. J.; Fox, J. M.; Shaw, J. T. Synthesis of Benzodihydrofurans by Asymmetric C–H Insertion Reactions of Donor/Donor Rhodium Carbenes. *Chem. - A Eur. J.* **2017**, *23* (49), 11843–11855.

(8) Bergstrom, B. D.; Nickerson, L. A.; Shaw, J. T.; Souza, L. W. Transition Metal Catalyzed Insertion Reactions with Donor/Donor Carbenes. *Angew. Chemie - Int. Ed.* **2021**, *60* (13), 6864–6878.

(9) Soldi, C.; Lamb, K. N.; Squitieri, R. A.; González-López, M.; Di Maso, M. J.; Shaw, J. T. Enantioselective Intramolecular C-H Insertion Reactions of Donor-Donor Metal Carbenoids. *J. Am. Chem. Soc.* **2014**, *136* (43), 15142–15145.

(10) Ma, J.; Zhang, L.; Zhu, S. Enynal/Enynone: A Safe and Practical Carbenoid Precursor. *Curr. Org. Chem.* **2016**, *20* (1), 102–118.

(11) Musthapa, I.; Latip, J.; Takayama, H.; Juliawaty, L. D.; Hakim, E. H.; Syah, Y. M. Prenylated Flavones from Artocarpus Lanceifolius and Their Cytotoxic Properties against P-388 Cells. *Nat. Prod. Commun.* **2009**, *4* (7), 927–930.

(12) Suhartati, T.; Achmad, S. A.; Aimi, N.; Hakim, E. H.; Kitajima, M.; Takayama, H.; Takeya, K. Artoindonesianin L, a New Prenylated Flavone with Cytotoxic Activity from Artocarpus Rotunda. *Fitoterapia* **2001**, *72* (8), 912–918.

(13) Cao, J. Q.; Tian, H. Y.; Li, M. M.; Zhang, W.; Wang, Y.; Wang, L.; Ye, W. C. Rearranged Phloroglucinol-Monoterpenoid Adducts from Callistemon Rigidus. *J. Nat. Prod.* **2018**, *81* (1), 57–62.

(14) Wu, L.; Zhang, Y. L.; Wang, X. B.; Zhang, Y. M.; Yang, M. H.; Luo, J.; Kong, L. Y. Viminalins A-O: Diverse [3+2] Hybrids of Acylphloroglucinol and α-Phellandrene from the Fruits of Callistemon Viminalis. *Tetrahedron* **2017**, *73* (8), 1105–1113.

(15) Yoshinori, K.; Katsumi, K.; Tsutomu, T.; Tadaaki, O.; Takashi, Y.; Kazuhiro, O.; Seiichi, S.; Noboru, S.; Hiromichi, S.; Tomio, O.; Toshiaki, O.; Yukihiro, O.; Kimiyuki, S.; Yoshio, T.; Mikio, F.; Yasumi, U. Indole Derivatives, Salts Thereof and Heart Affection Therapeutic Agent Comprising the Same. EP19940117102 19941028, 1995.

(16) Uemura, H.; Sakamoto, N.; Nakaya, H. Electropharmacological Effects of UK-1745, a Novel Cardiotonic Drug, in Guinea-Pig Ventricular Myocytes. *Eur. J. Pharmacol.* **1999**, *383*(3), 361–371. https://doi.org/10.1016/S0014-2999(99)00651-2.

(17) Shigenori, O.; Yasuyoshi, A.; Kouki, K.; Masahiro, O.; Makaki, S. Benzofuran Derivatives, Process for the Preparation of the Same and Uses Tehreof. JP19980345355 19981204, 2000.

(18) Taber, D. F.; Petty, E. H.; Raman, K. Enantioselective Ring Construction: Synthesis of (+)-α-Cuparenone. *J. Am. Chem. Soc.* **1985**, *107* (1), 196–199.

(19) Doyle, M. P.; Kalinin, A. V.; Ene, D. G. Chiral Catalyst Controlled Diastereoselection and Regioselection in Intramolecular Carbon-Hydrogen Insertion Reactions of Diazoacetates. *J. Am. Chem. Soc.* **1996**, *118* (37), 8837–8846.

(20) Nakamura, E.; Yoshikai, N.; Yamanaka, M. Mechanism of C-H Bond Activation/C-C Bond Formation Reaction between Diazo Compound and Alkane Catalyzed by Dirhodium Tetracarboxylate. *J. Am. Chem. Soc.* **2002**, *124* (24), 7181–7192.

(21) Singha, S.; Buchsteiner, M.; Bistoni, G.; Goddard, R.; Furstner, A. A New Ligand Design Based on London Dispersion Empowers Chiral Bismuth − Rhodium Paddlewheel Catalysts. *J. Am. Chem. Soc.* **2021**, *143*, 5666–5673.

(22) Kong, L.; Han, X.; Chen, H.; Sun, H.; Lan, Y.; Li, X. Rhodium(II)-Catalyzed Regioselective Remote C − H Alkylation of Protic Indoles. *ACS Catal.* **2021**, *11*, 4929-4935.

(23) Fukuto, J. M.; Jensen, F. R. Mechanisms of SE2 Reactions: Emphasis on Organotin Compounds *Acc. Chem. Res* **1983**, *16*, 177-184.

(24) Tantillo, D. J. Recent excursions to the borderlands between the realms of concerted and stepwise: Carbocation cascades in natural products biosynthesis *J. Phys. Org. Chem.* **2008**, *21*, 561-570.

(25) Wang, J.; Chen, B.; Bao, J. Electronic Effects of Rh(II)-Mediated Carbenoid Intramolecular C-H Insertion: A Linear Free Energy Correlation Study. *J. Org. Chem.* **1998**, *63* (6), 1853–1862.

(26) Drago, R. S.; Tanner, S. P.; Richman, R. M.; Long, J. R. Quantitative Studies of Chemical Reactivity of Tetra-Yu-Butyrato-Dirhodium(II) Complexes. *J. Am. Chem. Soc.* **1979**, *101* (11), 2897–2903.

(27) Trindade, A. F.; Coelho, J. A. S.; Afonso, C. A. M.; Veiros, L. F.; Gois, P. M. Fine tuning of dirhodium(II) complexes: Exploring the axial modification *ACS Catal.* **2012**, *2*, 370–383.

(28) Adly, F. On the Structure of Chiral Dirhodium(II) Carboxylate Catalysts: Stereoselectivity Relevance and Insights *Catalysts*, **2017**, *7*, 347.

(29) Carpenter, B. K. Energy disposition in reactive intermediates *Chem. Rev.* **2013**, *113*, 7265-7286.

(30) Plata, R. E.; Singleton, D. A. A Case Study of the Mechanism of Alcohol-Mediated Morita Baylis–Hillman Reactions. The Importance of Experimental Observations *J. Am. Chem. Soc.* **2015**, *137*, 3811-3826.

(31) Álvarez-Moreno, M.; de Graaf, C.; Lopez, N.; Maseras, F.; Poblet, J.M.; Bo, C. *J. Chem. Inf. Model*. **2015**, *55*, 95-103.

(32) Dishman, S.N.; Laconsay, C.J.; Fettinger, J.C.; Tantillo, D.J.; Shaw, J.T. Divergent Stereochemical Outcomes in the Insertion of Donor/Donor Carbenes into the C–H Bonds of Stereogenic Centers. *ChemRxiv*. **2021**. DOI: 10.33774/chemrxiv-2021-h06nc.

SYNOPSIS TOC (Word Style "SN_Synopsis_TOC"). If you are submitting your paper to a journal that requires a synopsis graphic and/or synopsis paragraph, see the Instructions for Authors on the journal's homepage for a description of what needs to be provided and for the size requirements of the artwork.

Authors are required to submit a graphic entry for the Table of Contents (TOC) that, in conjunction with the manuscript title, should give the reader a representative idea of one of the following: A key structure, reaction, equation, concept, or theorem, etc., that is discussed in the manuscript. Consult the journal's Instructions for Authors for TOC graphic specifications.